

ANALYSIS OF PROMPT DECAY EXPERIMENTS FOR ADS REACTIVITY MONITORING AT VENUS-F FACILITY

**S. Chabod¹, X. Doligez², G. Lehaut³, A. Billebaud¹, J.-L. Lecouey³, F.-R. Lecolley³, N. Marie³,
A. Kochetkov⁴, W. Uyttenhove⁴, G. Vittiglio⁴, J. Wagemans⁴,
F. Mellier⁵, G. Ban³, H.-E. Thyébault¹, D. Villamarin⁶**

¹Laboratoire de Physique Subatomique et de Cosmologie, CNRS-IN2P3/UJF/INPG, France

²Institut de Physique Nucléaire d'Orsay, CNRS-IN2P3/Univ. Paris Sud, France

³Laboratoire de Physique Corpusculaire de Caen, ENSICAEN/Univ. de Caen/CNRS-IN2P3, France

⁴StudieCentrum voor Kernenergie-Centre d'Etude de l'Energie Nucléaire, Belgium

⁵Commissariat à l'Energie Atomique et aux Energies Alternatives, DEN/DER/SPEX, France

⁶Centro de Investigaciones Energeticas MedioAmbientales y Tecnológicas, Spain

On behalf of the FREYA collaboration

Abstract

The GUINEVERE (EUROTRANS-IP FP6) and FREYA (FP7) projects address the main issue of ADS reactivity on-line monitoring. The latter aims at validating a methodology that consists in the combination of two approaches: (i) the time monitoring of the reactor power as well as the beam intensity (i.e. source intensity), that give access to the on-line relative fluctuations of the reactivity, $\rho(t)$, around a reference value; (ii) some calibration measurements, performed regularly, providing an absolute level of ρ . This absolute level – that may evolve with time too but slower – is used as a reference for the on-line relative measurements.

The calibration measurements are based on the analysis of the time decay of the reactor neutron population, $N(t)$, measured during programmed beam interruptions. Different analysis techniques can be applied, but most of them require analyzing both prompt and delayed neutron contributions (as the area method, *ibid.* Marie et al.). Consequently, to give precise results these techniques require the use of long beam interruptions, of several ms durations.

In this paper, we describe an innovative analysis method that relies only on the prompt component of the neutron decay. It can thus be applied to shorter beam interruptions, of a few tens of microseconds. The method, called integral k_p method as it allows the determination of the reactor prompt multiplication factor, is applied to the first experimental data taken at SCK-CEN VENUS-F facility, with promising preliminary results.

Introduction

Researches on Accelerator Driven Systems (ADS) gave birth to several experimental projects supported by the EURATOM Framework Programs. One of the main issues investigated is linked to the safety. In particular, the property of piloting a reactor thanks to the accelerator holds only if the core is far enough from the criticality. In a powerful core several phenomena could lead to an increase of reactivity (fuel evolution, Doppler effect...). It is then of paramount importance during operation of an ADS to be able to prove that it remains sub-critical in a given margin. The absolute reactivity measurement of a core is, however, not a trivial issue, especially in steady state operation, as the only available observable is the neutron flux (or more exactly fission rates in detectors). Moreover standard techniques to determine the reactivity of a sub-critical core must refer to a critical core, which is not a step foreseen in powerful systems. This issue has been investigated for the last 15 years, which have represented the time scale for preparing and exploiting two fast ADS mock-ups in Europe in dedicated experimental projects. In 2006, the GUINEVERE project joined the EUROTRANS Integrated Project (FP6) to carry on with the reactivity monitoring work started in the MUSE project (FP5) at the MASURCA reactor facility (CEA, France). The GUINEVERE (Generator of Uninterrupted Intense NEutron at the lead VENUS REactor) project (2006-2010) consisted first in achieving an innovative lead fast ADS mock-up at the VENUS facility (SCK-CEN, Belgium), with dedicated neutron source specifications. The exploitation of this mock-up for the reactivity monitoring methodology investigation goes on into the FREYA (Fast Reactor Experiments for hYbrid Applications) project, launched in 2011 in the FP7. The strategy chosen to monitor a sub-critical core reactivity combines two approaches: (i) the on-line monitoring of the relative fluctuations of the reactivity $\rho(t)$, thanks to the measurement of the ratio of the beam intensity to the reactor power; (ii) some calibration measurements, performed regularly, providing an absolute level of ρ . These absolute or calibration measurements are performed during beam interruptions and are based on the analysis of the time decay of the reactor neutron population, $N(t)$. In this paper, we focus on the prompt decay part of $N(t)$ and present a method to determine the prompt multiplication factor k_p , from which the k_{eff} can be inferred. The method is applied on Pulsed Neutron Source (PNS) measurements.

The VENUS-F facility

The VENUS-F facility (Fig. 1 left) is a zero power ADS mock-up and consists in the vertical coupling of the VENUS reactor (SCK-CEN, Mol, Belgium) with a deuteron accelerator GENEPI-3C. The deuteron ions are accelerated (220 keV) onto a tritiated target located at the reactor core centre, creating neutrons by $T(d,n)^4He$ reactions. The time structure of the beam can be chosen between three different modes: the pulsed mode (20 mA peak current over 1 μs , with a repetition rate bounded by 10Hz and 4 kHz), the continuous mode (with an intensity bounded by 100 μA and 1 mA), and the beam trip mode where beam interruptions (300 μs to a few ms) are made at a low frequency (a few tens to a few hundreds of Hz) in the continuous beam.

For the sub-critical experiments in the FEYA project, the VENUS-F reactor is loaded with 93 square fuel assemblies (FA) arranged in a cylindrical geometry, composed of 30% ^{235}U enriched metallic uranium (provided by CEA) and solid lead rodlets that mimic a fast system coolant. The fissile zone is surrounded axially and radially by a lead reflector. For mechanical reasons, the 12x12 assemblies are contained into a square stainless steel casing. The reactor is equipped with six safety rods (SF) with fuel followers, two control rods (CR) and one absorbent rod for rod drop experiments. The ending part of the accelerator is inserted into the core in a central hole corresponding to the size of 4 fuel assemblies. This sub-critical configuration, with the CRs at a height of 479.3 mm and the absorbent rod inserted is called the "SC1" level. The CRs' height is the one giving a critical core when

the four central FAs are added and the absorbent rod is withdrawn. A cross section view of the SC1 core is shown in Fig. 1 (right). More details on the VENUS-F facility can be found elsewhere [1]. The reactivity value of the SC1 core was found equal to -5.3 ± 0.23 \$ by the MSM method [2].

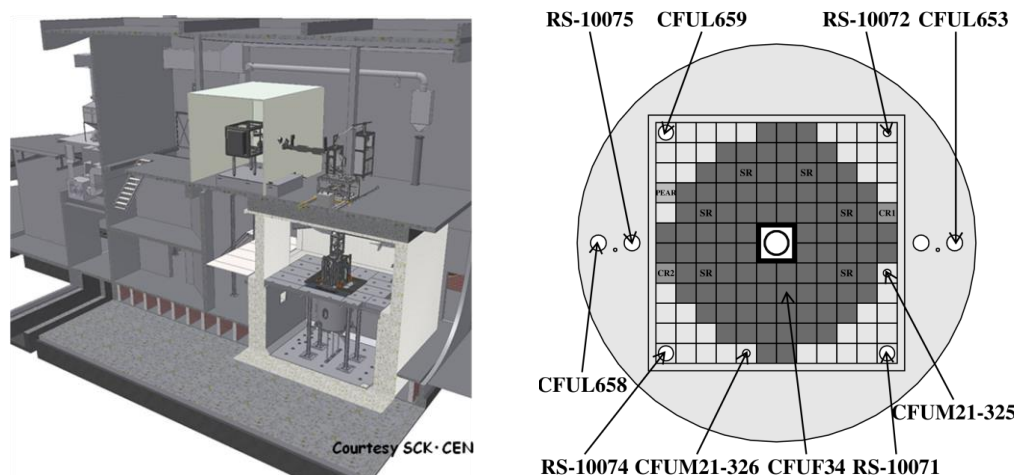


Figure 1: (left) the VENUS-F facility (SCK-CEN, Mol, B); (right) the sub-critical core SC1 (cross view) with detector locations.

Pulsed Neutron Source measurements

Measurements in the core consist in fission rate measurements performed with ten ^{235}U fission chambers having different efficiencies. The different types of detectors and their associated fissile deposits are summed-up in Table 1. Most of them are located in the reactor reflector, some of them being inside the casing (inner reflector) and a few of them being outside (outer reflector), as shown in Fig. 1 (right). One fission chamber is placed inside the core part composed of FAs. The pulsed neutron source measurements are performed with the accelerator in pulsed mode, at 200 Hz and in the SC1 configuration described above. The neutron source shape is close to a Gaussian with a FWHM of the order of 500 ns.

Table 1: Detector specifications.

Name	Type	Location	Deposit (content)	Approximate mass (mg)
D1	CFUL659	Inner reflector	^{235}U (~92%)	1000
D2	CFUL658	Outer reflector	^{235}U (~92%)	1000
D3	CFUL653	Outer reflector	^{235}U (~92%)	1000
D4	RS-10072	Inner reflector	^{235}U (~90%)	100
D5	RS-10071	Inner reflector	^{235}U (~90%)	100
D6	RS-10074	Inner reflector	^{235}U (~90%)	100
D7	RS-10075	Outer reflector	^{235}U (~90%)	100
D8	CFUF34	Fuel	^{235}U (100%)	1
D9	CFUM326	Inner reflector	^{235}U (~90%)	10
D10	CFUM325	Inner reflector	^{235}U (~90%)	10

Fission events are time stamped with a resolution of 20 ns by the GANDDALF data acquisition system designed for this program. The neutron source intensity is of the order of 10^6 neutrons per pulse. The time spectra obtained for each pulse are added and the Fig. 2 shows the final time spectra obtained for 8.36×10^6 neutron pulses for the ten detectors. At first glance we see the different detector efficiencies and if we have a closer look we observe that curve shapes gather as a function of detector locations.

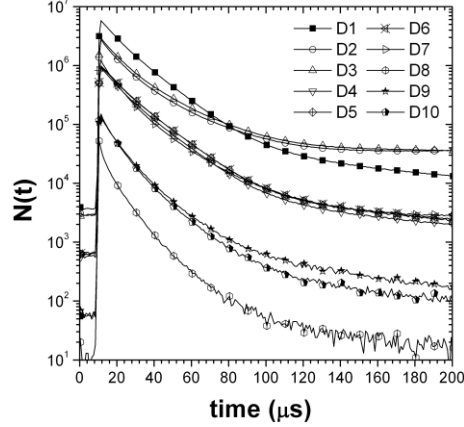


Figure 2: Raw Pulsed Neutron Source measurements obtained at 200 Hz in SC1 configuration.

Description of the k_p method

Number of neutrons born at a time t into a sub-critical reactor

Let us suppose we inject a number, $S(t)$, of source neutrons at a time $t \geq 0$ into a subcritical reactor. These neutrons, of generation 0, will propagate throughout the medium and, for a fraction of them, will induce fissions. The neutrons of generation 1, released by these first fissions, induce at their turn new fissions, initiating a fission chain that ultimately dampens due to the system sub-criticality. The number, $N_{n+1}(t)$, of neutrons of generation $n+1$ born at time t in the reactor can be related to the number, $N_n(t)$, of neutrons of generation n through a simple equation:

$$N_{n+1}(t) = k_p (P \otimes N_n)(t) = k_p \int_{\tau=0}^t N_n(t-\tau) P(\tau) d\tau, \quad \int_{\tau=0}^{+\infty} P(\tau) d\tau = 1. \quad (1)$$

In (1), symbol \otimes stands for the convolution product, k_p is the prompt multiplication factor. Function $P(\tau)$ is the intergeneration time distribution, i.e. the probability density that a newly born neutron induces a fission after a time τ . In this study, we suppose that the distribution $P(\tau)$ is independent of the generation number.

We want to calculate the number, $N(t)$, of neutrons that are generated in the reactor at time t by fissions. This number is given by the sum of all neutron generations: $N(t) = N_0(t) + N_1(t) + \dots + N_n(t) + \text{etc.}$ Thus, using relation (1) and observing that $N_0(t) = S(t)$, we obtain an equation that governs the time evolution of the neutron population $N(t)$:

$$N(t) = S(t) + k_p (P \otimes N)(t). \quad (2)$$

In this study, the neutron source pulse $S(t)$ is modelled by a Gaussian. Using Laplace transform, that transforms a convolution product into an algebraic one, we can reformulate (2):

$$L(N) = \frac{L(S)}{1 - k_p L(P)}, \quad L(f) = \int_{t=0}^{+\infty} e^{-pt} f(t) dt, \quad L(f \otimes g) = L(f)L(g). \quad (3)$$

An analytical solution of (3) can be obtained, and reads:

$$N(t) = S(t) + k_p (P \otimes S)(t) + k_p^2 (P \otimes P \otimes S)(t) + k_p^3 (P \otimes P \otimes P \otimes S)(t) + \dots \quad (4)$$

Providing we have a good knowledge of the intergeneration time distribution, $P(\tau)$, by using the integral equation (2) we are now able to calculate numerically the time evolution of the number, $N(t)$, of neutrons born at time t in a subcritical reactor.

The intergeneration time distribution $P(\tau)$

The $P(\tau)$ distribution can be computed using the MCNP transport code in a KCODE mode [3]. The results obtained for VENUS-F reactor are presented in Fig. 3 (left), alongside with an analytical distribution, $P_{PK}(\tau) = \exp(-\tau/\Lambda)/\Lambda$. The $P_{PK}(\tau)$ curve is the intergeneration time distribution obtained for the Point Kinetics hypothesis. Number Λ is the mean time elapsed between two fissions, equal to $0.5 \mu\text{s}$ in VENUS-F. As shown in Fig. 3, the Point Kinetics hypothesis is unable to reproduce the VENUS-F $P(\tau)$ shape, more specifically, its tail at large times. This tail is due to the VENUS-F lead reflector and concrete, which act as pools returning moderated neutrons back to the fissile core after several tens of μs .

For a given reactor, we indicate that the distribution $P(\tau)$ is insensitive to: (i) reasonable changes in reactivity. Indeed, the differences between two $P(\tau)$ curves computed for $k_{eff} = 0.964$ and 0.994 are negligible; (ii) choice of the nuclear cross-sections database; (iii) reasonable changes in core geometry [4,5]. The insensitivity of the $P(\tau)$ function to these changes is a cornerstone of the k_p method. Therefore, by computing a single $P(\tau)$ distribution and by folding it using (4), we can simulate the prompt decays occurring in a reactor for a large range of k_p configurations.

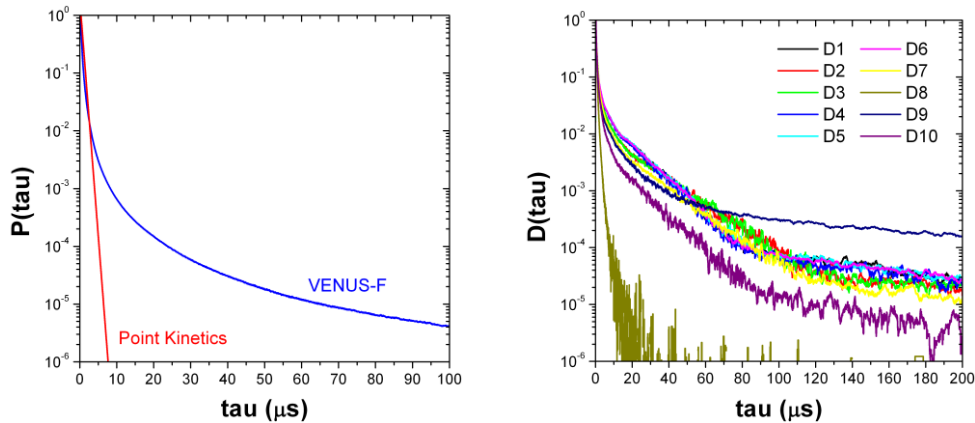


Figure 3: (left) Distribution $P(\tau)$ obtained for the VENUS-F reactor compared with the predictions of Point Kinetics; (right) Distributions $D(\tau)$ obtained for the D1 to D10 detectors.

Number of events, $M(t)$, detected at time t in a fission chamber

In our experiment, however, the physical observable is not the number $N(t)$ of fissions occurring in the reactor, but the number of counts measured in several fission chambers positioned inside the VENUS-F core and reflector (cf. Fig. 1). The theoretical number of counts, $M_{th}(t)$, recorded at time t in a detector can be related to the neutron population, $N(t)$, by introducing a new distribution called $D(\tau)$. Function $D(\tau)$ is the distribution of times elapsed between a fission occurring in the reactor and a fission occurring in the fissile deposit of the considered detector. Omitting the detector efficiency we have:

$$M_{th}(t) = (D \otimes N)(t). \quad (5)$$

Distribution $D(\tau)$ accounts for the transport of neutrons from the coordinates of fissions to the detector position. As a result: (i) the distribution $D(\tau)$ is more sensitive than the $P(\tau)$ distribution to the reactor geometry and composition; (ii) to obtain $D(\tau)$ with a sufficient statistics, more computer resources are required than what is needed to compute $P(\tau)$. For both reasons and according to MUSE conclusions, it is recommended to apply the k_p method preferentially to threshold detectors, such as fission chambers with ^{237}Np or pure ^{238}U deposits. For a threshold detector, indeed, the $D(\tau)$ function reduces to a Dirac, $\delta(\tau)$, since the time needed to transport MeV neutrons along a distance of about 1 m is negligible compared to the prompt decay time. Easing the need for $D(\tau)$ calculation and folding greatly facilitates in return the comparison of experimental to theoretical data.

Unfortunately, it is very difficult to get threshold fission chambers with an efficiency adapted to a zero power experiment. For these experiments, we only used conventional ^{235}U fission detectors that are sensitive to low energy neutrons and thus to the details of the neutron trajectories. In return, we were compelled to compute their $D(\tau)$ distributions, a task undertaken using MCNP code [3]. The results are presented in the right part of Fig. 3 for the detectors used in VENUS-F reactor.

Extraction of the k_p factor

By computing the distributions $P(\tau)$ and $D(\tau)$, then by using the theoretical background summarized in eq. (2) and (5), we are able to simulate the time evolutions, $M_{th}(t, k_p)$, of the count rates measured by our detectors, as a function of two parameters: (i) the time t ; (ii) the prompt multiplication factor k_p . By comparing this theoretical data with the experimental ones, $M_{exp}(t)$, we can infer the k_p value for the SC1 configuration.

Improvement of the k_p method

New methodology to compare the theoretical and experimental results $M_{th}(t, k_p)$ and $M_{exp}(t)$

As they have neither the same normalisation nor the same starting times, the theoretical and experimental count rates, $M_{th}(t, k_p)$ and $M_{exp}(t)$, cannot be directly compared. In the classical approach of the k_p method, this comparison is undertaken by calculating and then by comparing their logarithmic time derivatives [4,5]. However, this approach is highly sensitive to the statistical fluctuations occurring in the experimental $M_{exp}(t)$ curves, fluctuations that induce at their turn large fluctuations on the $M_{exp}(t)$ logarithmic derivatives [6]. To circumvent this issue, we propose a novel

estimator, $W(t)$, that relies on the integration of the $M(t)$ curves rather than on their derivation, since an integral is more continuous than a derivative. This estimator is one of the simplest, self-normalized, integral estimators that can be chosen, and is defined by:

$$W(t) = \frac{\int_{t'=t_{min}}^t M^2(t') dt'}{\left(\int_{t'=t_{min}}^t M(t') dt' \right)^2}. \quad (6)$$

In (6), the time t_{min} is a cut-off, used to reject the first 10 μs of the theoretical and experimental curves, sensitive to issues such as: (i) the source time shape, that is not perfectly Gaussian; (ii) the dead time effects, corrected in our study, but minor errors can still occur; (iii) the weight of the first generations of neutrons whose intergeneration time distributions are not strictly equal to $P(\tau)$; (iv) numerical transients: as the distribution $P(\tau)$ is given in the form of a histogram, we indeed note that the integral equation, (2), that governs the time evolution of the neutron population is mathematically equivalent to the equation giving the neutron flux in an infinite medium where the moderation is due to elastic collisions. The solution of (2) thus exhibits a short and artificial transient, identical to Placzek's one [7], during the first μs , that must be discarded.

Statistical errors on the theoretical and experimental estimators, $W_{th}(t)$ and $W_{exp}(t)$, respectively coming from: (theory) the MCNP statistical fluctuations on $P(\tau)$ and $D(\tau)$ histograms; (experiment) the statistics of the detector count rates, can be computed using a Monte-Carlo procedure (Gaussian sampling within the error bars). As the $W(t)$ fluctuations were proven to be normally distributed, we can use a χ^2 test to compare the theoretical and experimental data, in order to determine the value of the prompt multiplication factor k_p :

$$\left(\chi^2 / n \right) (k_p) = \frac{1}{N-1} \sum_{i=1}^N \frac{\left(W_{exp}(t_i) - W_{th}(t_i, k_p) \right)^2}{\varepsilon_{W_{exp}}(t_i)^2 + \varepsilon_{W_{th}}(t_i, k_p)^2} \quad (7)$$

where N is the number of points, t_i , used to compare the $W_{th}(t, k_p)$ and $W_{exp}(t)$ data. Functions $\varepsilon_W(t)$ are the error bars on $W(t)$. We had not enough time to compute the theoretical errors, $\varepsilon_{W_{th}}(t, k_p)$, for each $W_{th}(t, k_p)$ curves, since the Monte-Carlo procedure requires large amount of computer resources. For this study, we had thus to omit them.

Blind test of the analysis methodology

To investigate: (i) the precision of the numerical procedure used to solve the integral equation (2); (ii) the ability of the integral estimator, $W(t)$, to constrain the k_p value at the 100 pcm level, we performed a blind test on a simpler, but still representative, case than the VENUS-F reactor. We considered a distribution $P_{test}(\tau)$ given by the sum of two exponentials of different characteristic times: a short one to model a fissile core, a longer one to model the influence of a reflector:

$$P_{test}(\tau) = Ae^{-\alpha\tau} + Be^{-\beta\tau}, \quad L(P_{test}) = \frac{A}{p + \alpha} + \frac{B}{p + \beta} \quad (8)$$

with $A = 2.4 \mu\text{s}^{-1}$, $B = 2.2 \times 10^{-5} \mu\text{s}$, $\alpha = 2.4 \mu\text{s}^{-1}$, $\beta = 1.8 \times 10^{-2} \mu\text{s}$. Parameters A , B , α , β were chosen: (i) to mimic the long tail of the VENUS-F $P(\tau)$ distribution, see Fig. 3; (ii) to obtain a mean

intergeneration time, Λ , similar to the $0.5 \mu\text{s}$ of VENUS-F; (iii) to preserve the normalisation of $P_{test}(\tau)$. We then transformed the distribution $P_{test}(\tau)$ into a histogram and artificially noised it to mimic the statistical fluctuations observed on MCNP simulations. The resulting curve is shown in Fig. 4. Finally, we numerically solved the integral equations (2) and (5), for k_p factors ranging from 0.949 to 0.951 by steps of 10 pcm, to create a set of theoretical count rates, $M_{th}(t, k_p)$, for a threshold detector (reminder: $D(\tau) = \delta(\tau)$ for a threshold detector).

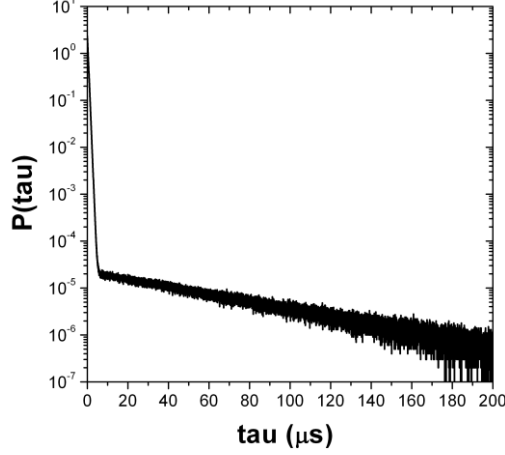


Figure 4: Simplified intergeneration time distribution, $P_{test}(\tau)$, used for the methodology blind test.

In a second step, we generated a set of pseudo-experimental data. For an instantaneous source pulse, $S(t) = \delta(t)$, the time evolution of the count rate in a threshold detector obeys to:

$$L(M) = \frac{L(D)L(S)}{1 - k_p L(P)} = \frac{1}{1 - k_p L(P)}. \quad (9)$$

Using expression (8), transforming the ratio $1/(1 - k_p L(P))$ into a sum of partial fractions, then inverting the Laplace transform leads to the foreseen detector count rate:

$$\begin{aligned} M(t) &= \delta(t) + K_1 e^{p_1 t} + K_2 e^{p_2 t} \\ p_1 &= \frac{1}{2} [k_p (A + B) - (\alpha + \beta) + \gamma], \quad p_2 = \frac{1}{2} [k_p (A + B) - (\alpha + \beta) - \gamma] \\ K_1 &= (p_1 + \alpha)(p_1 + \beta) / \gamma, \quad K_2 = -(p_2 + \alpha)(p_2 + \beta) / \gamma \\ \gamma &= \sqrt{(A + B)^2 k_p^2 - 2(A - B)(\alpha - \beta)k_p + (\alpha - \beta)^2} \end{aligned} \quad (10)$$

We note that a double-exponential intergeneration time distribution leads to a neutron population varying as a double-exponential. The computation of the characteristic times, $1/p_1$ and $1/p_2$, as a function of k_p gives interesting results. For instance, we note that $p_1 \rightarrow 0$ when $k_p \rightarrow 1$; the double-exponential behaviour of $N(t)$ vanishes when the reactor approaches criticality. The set of pseudo-experimental data was thus generating using expression (10) for $k_p = 0.95$. The $M_{exp}(t)$ curve was transformed into a histogram and noised to reproduce the statistical fluctuations observed on VENUS-F detectors. The $M_{exp}(t)$ curve is shown in Fig. 5, alongside with the theoretical curve $M_{th}(t, k_p = 0.95)$.

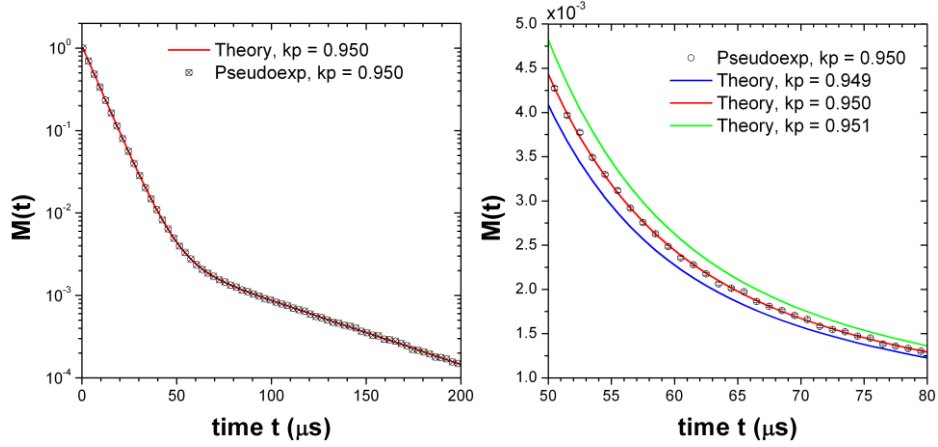


Figure 5: Pseudo-experimental count rates (dots), $M_{exp}(t)$, obtained for $k_p = 0.95$, compared to theoretical results (lines), $M_{th}(t, k_p = 0.949-0.951)$, obtained by folding the noised distribution $P_{test}(\tau)$.

Finally, we computed the theoretical and experimental estimators $W_{th}(t, k_p)$ and $W_{exp}(t)$. The statistical fluctuations on the $P_{test}(\tau)$ and $M_{exp}(t)$ curves were propagated using a Monte-Carlo method (Gaussian sampling within the error bars) to obtain the error bars on W_{th} and W_{exp} . The $W_{th}(t, k_p)$ and $W_{exp}(t)$ curves are shown in Fig. 6 (left). We then used a χ^2 test to compare the theoretical and experimental data. The evolution of the reduced χ^2 , given in (7), as a function of k_p is shown in Fig. 6 (right). Despite the large statistical fluctuations generated on $P_{test}(\tau)$ and $M_{exp}(t)$, the χ^2 analysis leads to a precise value of k_p , equal to 0.949974 ± 1.4 pcm. This result is compatible with the value, $k_p = 0.95$, used to generate the pseudo-experimental set of data.

The blind test thus gives two important results: (i) the numerical errors, resulting from the numerical resolution of equation (2), are responsible for a systematic error on k_p lower than 5 pcm. This is affordable; (ii) even when the $M_{th}(t, k_p)$ and $M_{exp}(t)$ curves are plagued by large statistical fluctuations, the estimator $W(t)$ has a resolution power high enough to separate k_p values differing from each other by less than 5 pcm. With these conclusions, the analysis methodology is validated.

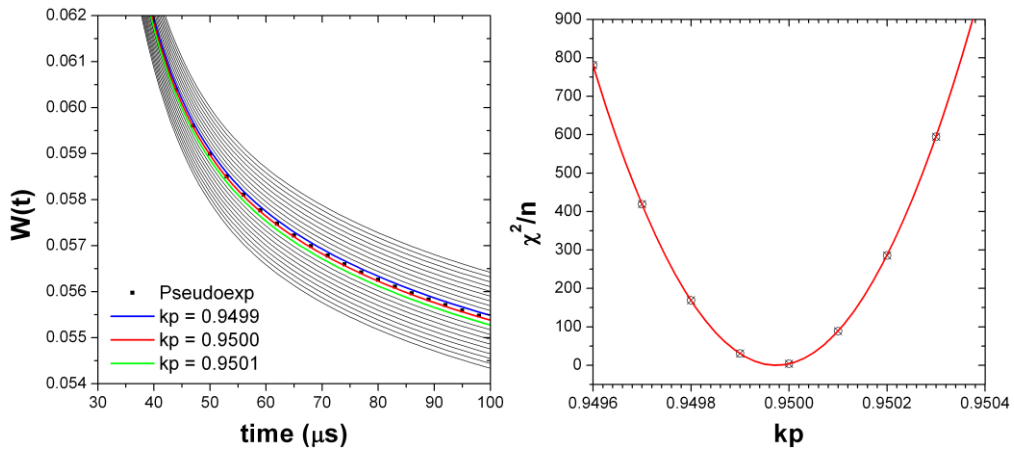


Figure 6: (left) experimental estimator $W_{exp}(t)$ (dots) and theoretical estimators $W_{th}(t, k_p)$ (lines) as a function of time. The theoretical curves $W_{th}(t, k_p)$ are calculated for k_p values ranging from 0.949 to 0.951 by 10 pcm steps; (right) evolution of the reduced χ^2 (7) as a function of k_p .

Analysis of VENUS-F experimental data and conclusions

The methodology detailed in this work is applied to the PNS measurements described above. The time spectra are corrected for dead time effects. The delayed neutron component, assumed constant over the few tens of μs after the pulse, is subtracted. The experimental estimators, $W_{exp}(t)$, are compared with arrays of theoretical estimators, $W_{th}(t, k_p)$, computed for k_p values ranging from 0.93 to 0.97 by steps of 50 pcm. The reduced χ^2 , (7), are calculated for each detector as a function of the prompt multiplication factor, k_p , and the time, T , elapsed since the neutron pulse injection. Their contour plots are shown in Fig. 7 for three representative detectors. For each detector, the k_p value and its error bar are given by the width of the $\chi^2 \leq \chi^2_{\min} + 1$ area. The k_p to k_{eff} correspondence is done with the relation $k_{eff} = k_p / (1 - \beta_{eff})$, using a β_{eff} value of 722 pcm calculated with ERANOS [8]. Finally, the reactivities ρ obtained for the detectors D1 to D10 are gathered in Table 2 and Fig. 8. Except for D2 and D3 detectors, we note that the preliminary results obtained with the improved k_p method are compatible with the reference MSM value, calculated in [2]. The D2 and D3 detectors are located outside the core casing, in an area that is up to now not correctly simulated. D2 and D3 mitigated results emphasize the need for threshold fissile deposits when the detectors have to be positioned far away from the core, as they are more sensitive to the modelling of neutron transport.

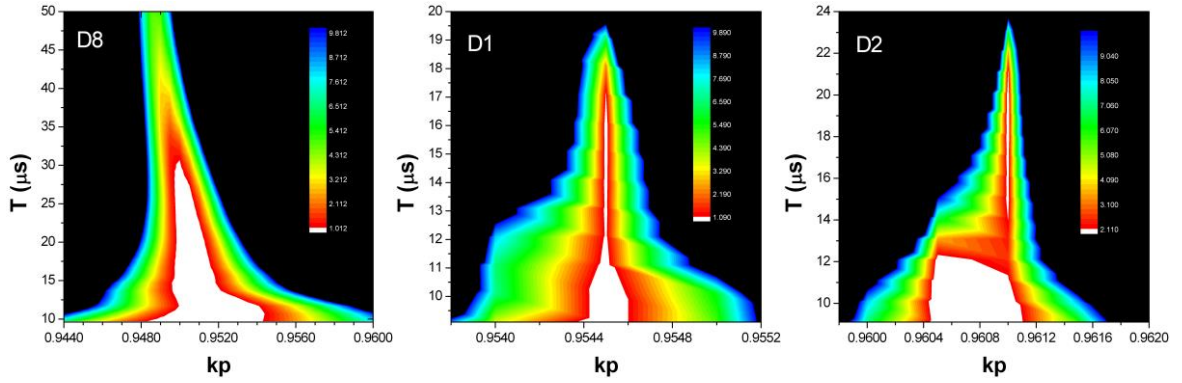


Figure 7: Contour plots of the reduced χ^2 as a function of k_p and T , time elapsed since the neutron pulse, for three representative detectors: D8 (in fuel), D1 (inner reflector), D2 (outer reflector).

Table 2: Preliminary results of the improved k_p method applied to the PNS experiments performed at VENUS-F reactor. The last line gives the reference MSM result [2].

Detector	k_p	k_{eff}	$-\rho$, in $\$$
D1	0.9543 – 0.9547	0.9612 – 0.9616	5.52 – 5.58
D2	0.9598 – 0.9617	0.9668 – 0.9687	4.48 – 4.76
D3	0.9624 – 0.9638	0.9694 – 0.9708	4.16 – 4.37
D4	0.9539 – 0.9559	0.9608 – 0.9629	5.34 – 5.65
D5	0.9563 – 0.9575	0.9633 – 0.9645	5.10 – 5.28
D6	0.9549 – 0.9565	0.9618 – 0.9635	5.25 – 5.49
D7	0.9534 – 0.9561	0.9603 – 0.9631	5.31 – 5.72
D8	0.9475 – 0.9554	0.9544 – 0.9624	5.42 – 6.62
D9	0.9509 – 0.9568	0.9578 – 0.9638	5.21 – 6.10
D10	0.9524 – 0.9580	0.9593 – 0.9650	5.03 – 5.87
MSM			5.30 ± 0.23

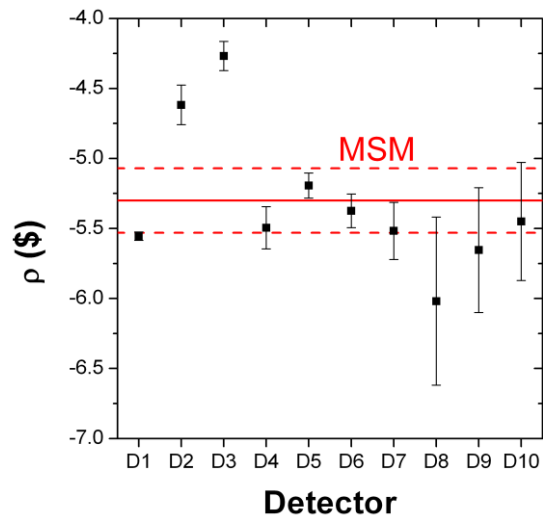


Figure 8: Reactivities ρ in dollars obtained with the improved k_p method for the ten detectors used at VENUS-F facility (squares). The results are compared with the MSM value (horizontal solid line) and its uncertainty (dashed lines).

Acknowledgements

This work is partially supported by the 6th and 7th Framework Programs of the European Commission (EURATOM) through the EUROTRANS-IP contract # FI6W-CT-2005-516520 and FREYA contract # 269665, and the French PACEN program of CNRS. The authors want to thank the VENUS reactor and GENEPI-3C accelerator technical teams for their help and support during experiments. They are also very grateful to the physics control service of SCK-CEN.

References

1. A. Billebaud et al., "The GUINEVERE Project for Accelerator Driven System Physics", Proceedings of Global 200, Paris, France (September 6-11, 2009).
2. J.-L. Lecouey et al., *In preparation (2013)*
P. Blaise, F. Mellier and P. Fougeras, IEEE Trans. Nucl. Science 58 3 (2011) 1166-1176.
3. MCNP - A General Monte Carlo N-Particle Code, Version 5, LA-ORNL, RSICC
LA-UR-03-1987, Los Alamos National Laboratory (2003).
4. F. Perdu et al., Prog. in Nucl. Energy, 42 (2003) 107.
5. J. Vollaire, "L'expérience MUSE-4 : Mesure des paramètres cinétiques d'un système sous-critique", PhD thesis, Grenoble INP (2004).
6. H.E. Thyébault et al., "The GUINEVERE Experiment: first PNS measurements in a lead moderated sub-critical fast core", Proceedings of International Congress on the Advances in Nuclear Power Plants (ICAPP'12), Chicago, USA (June 24-28, 2012).
7. G. Placzek, Phys. Rev. 69 (1946) 423.
8. M. Carta, ENEA, *private communication* (2011).